

Development of Enhanced, Permanently-Installed, Neutron Activation Diagnostic Hardware for NIF

E R Edwards¹, D R Jedlovec², J A Carrera², and C B Yeamans²

¹University of California, Berkeley, Berkeley, CA, USA

²Lawrence Livermore National Laboratory, Livermore, CA, USA

E-mail: edwards76@llnl.gov

Abstract. Neutron activation diagnostics are baseline neutron yield and flux measurement instruments at the National Ignition Facility. Up to 19 activation samples are distributed around the target chamber. Currently the samples must be removed to be counted, creating a 1-2 week data turn-around time and considerable labor costs. An improved system consisting of a commercially available LaBr₃(Ce) scintillator and Power over Ethernet electronics is under development. A machined zirconium-702 cap over the detector is the activation medium to measure the ⁹⁰Zr(n,2n)⁸⁹Zr reaction. The detectors are located at the current neutron activation diagnostic sites and monitored remotely. Because they collect data in real time yield values are returned within a few hours after a NIF shot.

1. Introduction

Neutron Activation Diagnostics (NADs) are used at the National Ignition Facility (NIF) to measure the neutron yield by activating a material through neutron reactions and measuring the γ -rays from the subsequent decay [1]. 19 Flange-NADs (FNADs) are distributed around the NIF target chamber to measure the spatial distribution of the yield. The FNADs are Zr pucks that measure the neutron flux at each location using the reaction ⁹⁰Zr(n,2n)⁸⁹Zr. The ⁸⁹Zr has a 78.41 hr half life [2] and emits a 909 keV γ -ray. This reaction has a 12.1 MeV threshold and therefore is sensitive only to 14.1 MeV primary DT neutrons. Currently they must be removed from the NIF target bay after each shot for counting, which is both time and labor intensive.

Two LaBr₃(Ce) scintillation detectors (Figure 1) were placed in the NIF target chamber at two of the current FNAD locations (Figure 2) [3]. Each detector receives its power from a Power over Ethernet (PoE) cable, which also transfers the data to the control room. The data is collected in list mode, which means that each event is recorded as a channel (energy) with a timestamp. Instead of a Zr puck, a Zr cap is placed over the crystal. The first detector has been in the target bay for 18 high-yield and many low-yield shots as of November 2015 and shows no signs of performance degradation from radiation damage. A yield measurement is returned in less than 8 hours.

2. ⁸⁹Zr ground state

Histograms are made by summing the number of events in each channel within a set time range (Figure 3). The time bin is chosen depending on the half life of the isotope of interest (30 minutes for ⁸⁹Zr). Many of these histograms are created and stacked together to show the spectrum as a function of time (Figure 5a). Energy and time are the axes and the colors represent the number of counts in each



energy/time bin. Since all of the original data remains unchanged, shorter or longer time intervals can be used in the post-processing to highlight certain features of the spectrum.



Figure 1. Lanthanum bromide detector at an FNAD port [4].

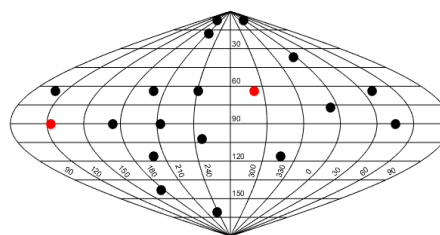


Figure 2. Current locations of the 19 Flange-NADs. The two prototype locations are shown in red.

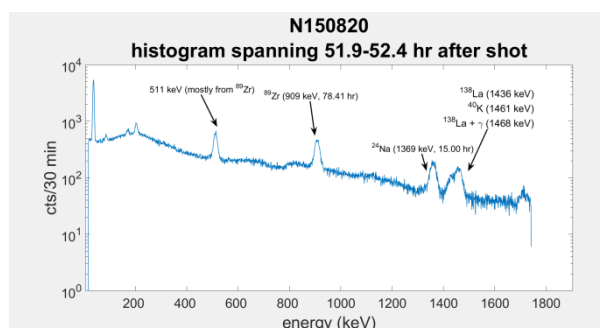


Figure 3. A histogram spanning a 30-minute interval starting 51.9 hr after N150820-003. Many of these histograms are stacked in time to form Figure 5a.

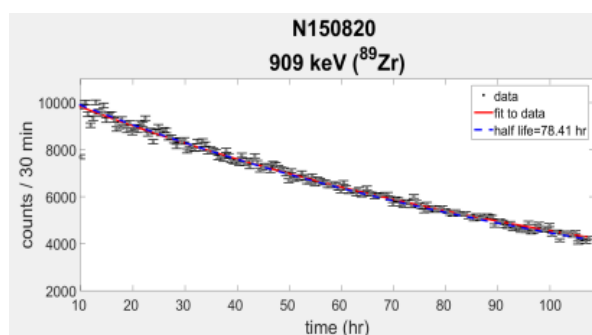


Figure 4. An energy range can be selected for a region surrounding a particular photopeak. Then the counts in the peak at each time interval are plotted as a function of time, and fit with an exponential. The resulting equation can be used to extrapolate the activity at shot time, which is used to find the yield.

The isotopes are identified by the energy and half lives of the photopeaks. To find the half life, an energy range surrounding the 909 keV peak is selected and the peak is fit. The peak area is plotted in time and an exponential decay is fit (Figure 4). The known ^{89}Zr half life of 78.41 hr is used, so the fit value is only a check. To calculate the neutron yield, the decay curve of ^{89}Zr is extrapolated to time zero using time bins of 30 minutes. Since the calibration is linear (Eq. 1 in [1]), the equation of the line can be used to convert counts to yield (Figure 8). The real-time system has shown that it is a viable replacement for a single FNAD position.

3. $^{89\text{m}}\text{Zr}$: Neutron Isomeric Ratio Detector (NIRD)

Neutrons can also activate ^{90}Zr to form the metastable state $^{89\text{m}}\text{Zr}$, which decays primarily by a 588 keV γ -ray with a half life of 4.18 minutes (Figures 9 and 10). It is not possible to observe it with the current FNAD system because the $^{89\text{m}}\text{Zr}$ has completely decayed by the time the FNAD pucks are recovered. It is sometimes observed with the LaBr_3 detectors. After each shot the activation of materials in the target chamber and electrons from β^- decays from activated La and Br within the detector create a high background that dominates the spectrum until it decays. After higher-yield ($>10^{15}$) shots the background is so high that none of the 588 keV γ -ray is visible. By the time the background has decayed, $^{89\text{m}}\text{Zr}$ has also completely decayed. However, part of the $^{89\text{m}}\text{Zr}$ decay is visible after medium-yield ($1\text{-}5 \times 10^{14}$) shots (Figure 6) and when the detector is placed far (28 m) from the neutron source in a shielded alcove (Figure 7). Because the cross section for producing ^{89}Zr and $^{89\text{m}}\text{Zr}$ depends on neutron energy, the observed $^{89\text{m}}\text{Zr}/^{89}\text{Zr}$ ratio could be used to determine the bulk

motion of the neutron source [5]. However, the high background prevents a precise measurement of ^{89m}Zr at this time.

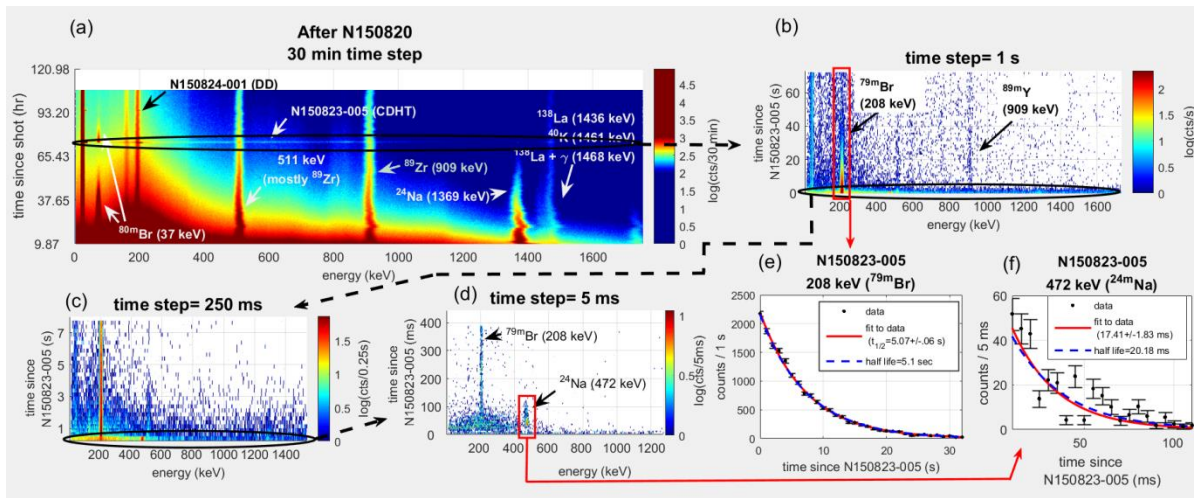


Figure 5. The detector continued running many days after N150820-003 and observed shots N150823-005 and N150824-001. Since the data is stored as a list of times and channels, it can be processed using varying time bins. Here the time bins were used to focus on N150823-005. By taking smaller and smaller time steps, different isotopes are observed (5a-5d). In 5a, the post-shot background has decayed enough so the natural radioactivity of ^{138}La in the detector is visible. 5e and 5f show the decays from ^{89m}Br and ^{24m}Na that can be observed.

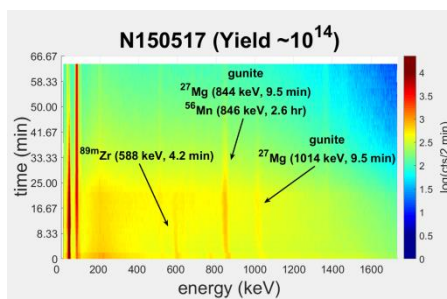


Figure 6. Example of ^{89m}Zr visible after a medium-yield shot, with detector on an FNAD port.

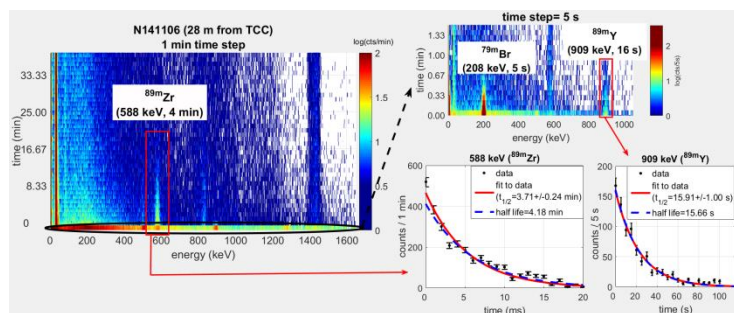


Figure 7. The background in the neutron alcove at 28 m and behind a shield wall is much lower, making it possible to see short-lived isotopes.

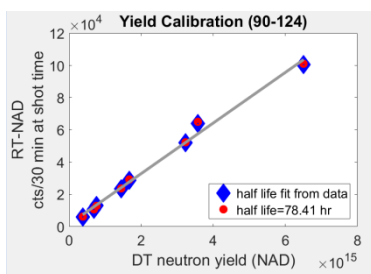


Figure 8. RT-NAD response calibration to yield.

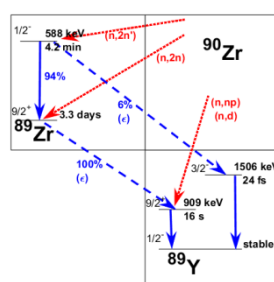


Figure 9. Reactions and decays in Zr and Y.

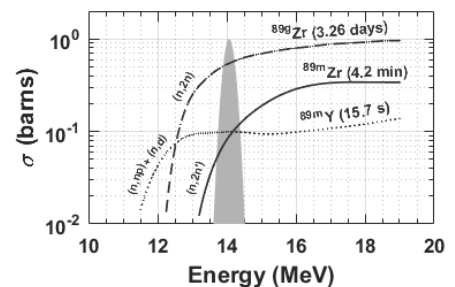


Figure 10. Neutron reactions on ^{90}Zr with DT neutron spectrum for reference. Cross sections from [6]-[10].

4. Short-lived isotopes: ^{89m}Y , ^{24m}Na , ^{79m}Br

Short-lived isotopes are observed when the detector is turned on before they have completely decayed, which for the shortest ones means the detector has to run through the shot. Furthermore, the background level must be low enough to see the signal. So far the short-lived isotopes have not been analysed in depth but they have the potential to be used to resolve the low-energy neutron spectrum. For example, the threshold for the $^{27}\text{Al}(n,\alpha)^{24}\text{Na}$ reaction is ~ 4.5 MeV but $^{79}\text{Br}(n,n')^{79m}\text{Br}$ is only ~ 210 keV. Reactions with low enough thresholds can also be used on DD shots to estimate the yield. A shot with mid- 10^{14} yield or higher causes a recoverable upset, and the detector cannot be restarted in time to catch the shortest-lived isotopes. Lower yield shots usually do not upset the detector.

The 909 keV γ -ray associated with ^{89}Zr decay is the relaxation of ^{89m}Y , which has a 16 s half life. Compared to the decay time of ^{89}Zr the half life of ^{89m}Y is negligible. The decay of ^{89m}Y produced directly by $^{90}\text{Zr}(n,np)^{89m}\text{Y}$ or $^{90}\text{Zr}(n,d)^{89m}\text{Y}$ (Figures 9 and 10) can be observed when it is produced in a short time (Figures 5b and 7).

One example of running through shots occurs after N150820-003 ($Y_n=7*10^{14}$). The detectors were restarted after the DT shot but ran through N150823-005 (3 days later), which had a DT yield of $\sim 10^{12}$, and N150824-001 (4 days later, $Y_{DD}=5.2*10^{10}$). N150823-005 was an opportunity to observe very short-lived isotopes since the activation background was low. ^{24m}Na ($t_{1/2}=20$ ms) is produced by the (n,α) reaction on ^{27}Al .

^{79}Br is 51% of the natural Br that makes up the scintillator crystal. Inelastic neutron scatter reactions with thresholds above 210 keV create ^{79m}Br with a 5.1 s half life. This reaction has been observed for low yield shots and with the detector 28 m from TCC. Both ^{24m}Na and ^{79m}Br are good examples of the ability to see isotopes with extremely short half lives. N150823-005 also demonstrates the usefulness of being able to run constantly and to analyze the data any time post-shot.

5. Conclusions

The primary goal of developing a more efficient and functional alternative to FNADs is achieved with RT-NAD. A linear calibration between DT neutron yield and RT-NAD response has been demonstrated. Furthermore, very short-lived isomers are observed under certain conditions and have the potential to become additional diagnostics. There is a greater choice in material since the half life does not have the limitation of the current FNADs. Operation is more efficient since they do not have to be removed to be counted, and a yield value is returned within hours instead of days. In the future the cap can be replaced with a different material to study other neutron reactions: for example, to measure DD and TT yields.

References

- [1] Bleuel D *et al* 2012 *Rev. Sci. Instrum.* **83** 10D313
- [2] Singh B 2013 *Nuc. Data Sheets* **114** 1-208
- [3] Jedlovac D, Edwards E, Carrera J and Yeaman C 2015 *Proc. SPIE 9591, Target Diagnostics Physics and Engineering for Inertial Confinement Fusion IV* vol 9591 ed J Koch and G Grim (San Diego: SPIE)
- [4] Crane R 2015 *CNN* <http://www.cnn.com/videos/tech/2015/10/02/orig-zp-nuclear-fusion-power-pioneers.cnn/video/playlists/pioneers-orig/>
- [5] Yeaman C, Bleuel D and Bernstein L 2012 *Rev. Sci. Instrum.* **83** 10D315
- [6] Semkova V, Bauge E, Plompen A and Smith D 2010 *Nuc. Phys. A* **832** 149–69
- [7] Chadwick M *et al* 2011 *ENDF/B-VII.1*
- [8] Kanda Y 1972 *Nuc. Phys. A* **185** 177-195
- [9] Abboud A, Decowski P, Grochulski W, Marcinkowski A, Piotrowski J, Siwek K and Wilhelm Z 1969 *Nuc. Phys. A* **139** 42-56
- [10] Pavlik A, Winkler G, Vonach H, Paulsen A and Liskien H 1982 *J. Phys. G* **8** 1283-1299